Published in final edited form as:
Neuroimage. 2009 October 15; 48(1): 166–175. doi:10.1016/j.neuroimage.2009.05.026.

Characterization of Regional Heterogeneity in Cerebrovascular Reactivity Dynamics Using Novel Hypocapnia Task and BOLD fMRI

Molly G. Bright, B.S.[1,2], **Daniel P. Bulte, Ph.D.**[2], **Peter Jezzard, Ph.D.**[2], and **Jeff H. Duyn, Ph.D.**[1]

[1]Laboratory for Advanced MRI, Laboratory of Functional and Molecular Imaging, National Institute of Neurological Disorders and Stroke, National Institutes of Health, Bethesda, MD, USA

[2]Oxford Centre for Functional MRI of the Brain, Department of Clinical Neurology, University of Oxford, Oxford, UK

Abstract

We offer a new method for characterizing the magnitude and dynamics of the vascular response to changes in arterial gas tensions using noninvasive blood oxygenation level-dependent functional magnetic resonance imaging (BOLD fMRI) and paradigms appropriate for clinical settings. A novel respiratory task, “Cued Deep Breathing” (CDB), consisting of two consecutive cycles of cued breaths, has been developed to cause transient hypocapnia, and consequently a strong, short-lived BOLD signal decrease. Data from CDB hypocapnia paradigms and traditional breath-holding hypercapnia paradigms were analyzed on a voxelwise basis to map regional heterogeneity in magnitude and timing parameters. The tasks caused comparable absolute BOLD percent signal changes (~0.5-3.0% in gray matter) and both datasets suggested consistent regional heterogeneity in the response timing: parts of the basal ganglia, particularly the putamen, and bilateral areas of medial cortex reached their maximum signal change several seconds earlier than remaining cortical gray matter voxels. This phenomenon and a slightly delayed response in posterior cortical regions were present in group-maps of ten healthy subjects. An auxiliary experiment in different subjects measured end-tidal CO_2 changes associated with the new CDB task and quantitatively compared the resulting reactivity maps with those acquired using a traditional hypercapnia challenge of 4% CO_2 gas inspiration. The CDB task caused average end-tidal CO_2 decreases between 6.0±1.1 and 10.5±2.6 mmHg, with levels returning to baseline after approximately three breaths, giving evidence that the task indeed causes transient mild hypocapnia. Similarity between resulting reactivity maps suggest CDB offers an alternative method for mapping cerebrovascular reactivity.

Keywords

fMRI; reactivity; BOLD; dynamics; breath holding; hypocapnia; hypercapnia; deep breathing

Introduction

The complex network of neurons in the brain requires a well-orchestrated vascular system to ensure a steady supply of glucose and oxygen to the cells. The cerebro-vasculature has

Corresponding Author: Molly Bright FMRIB Centre Department of Clinical Neurology University of Oxford John Radcliffe Hospital Headington, Oxford OX3 9DU UNITED KINGDOM Email: molly.bright@clneuro.ox.ac.uk Telephone: +44 (0)7770 988453 Fax: +44 (0)1865 222717.

developed fine-tuned regulatory mechanisms to adapt to typical fluctuations in blood pressure, oxygen saturation, and other systemic factors. By adjusting vessel size, blood flow can be maintained at the appropriate level to sustain cell function and health. Various phenomena can cause autoregulation to be augmented or disrupted, however. For example, during neuronal activation the local vessels dilate to increase blood flow in order to meet the demand for oxygen and glucose needed for metabolism. An even stronger effect can be observed if potent vasoactive substances are administered. In 1948, Kety and Schmidt explored the powerful vasodilatory nature of carbon dioxide, and measured the effects of hyperventilation (hypocapnia) and inspiration of a CO_2 gas mixture (hypercapnia) on blood pressure, pH, heart rate, blood flow, and metabolism (Kety and Schmidt, 1948). With the advent of noninvasive imaging techniques that can measure these physiological changes, researchers can now routinely study “cerebrovascular reactivity” (CVR) and its applications in basic science and clinical diagnosis.

A typical protocol for measuring CVR in patients utilizes Transcranial Doppler (TCD) sonography to measure changes in blood flow velocity through the internal carotid arteries or middle cerebral artery during administration of vasoactive factors. Using TCD in conjunction with a breath holding challenge, which systemically elevates the levels of CO_2 in the blood, CVR measurements were shown to assist in the prediction of future ischemic events in asymptomatic patients following endarterectomy (Silvestrini, et al., 2000). Another recent study used TCD during acetazolamide administration (a vasodilatory drug) to predict the development of post-operative diffusion lesions, giving further support for CVR as a specific and sensitive clinical metric (Aso, et al., 2008). More recently, the development of blood oxygenation level-dependent (BOLD) functional magnetic resonance imaging (fMRI) has enabled whole-brain high-resolution characterization of CVR, using the concentration of deoxygenated hemoglobin as an intrinsic contrast agent (Ogawa, et al., 1990; Graham, et al., 1994). The level of deoxygenated hemoglobin is sensitive to changes in blood flow, volume, and metabolism. In 2003, BOLD fMRI in conjunction with breath holding was directly compared with Single Photon Emission Computed Tomography (SPECT) during acetazolamide administration in a study of CVR in patients with vascular abnormalities. The CVR maps were in good agreement, revealing heterogeneous responses in tissue regions with impaired vasculature, and the BOLD fMRI results were observed to be less ambiguous in diagnosing individual pathologies (Shiino, et al., 2003). These studies imply that BOLD measurement of cerebrovascular reactivity offers relevant diagnostic information and could be included in patient research and routine vascular assessments. They also show that patient populations can execute respiratory challenges in the MRI scanner environment with proper coaching and experiment design. A study by Thomason, *et al*. (2005) successfully implemented breath holding techniques in young children (aged 7-12 years) in order to study the effect of age on the magnitude and noise of the BOLD response, while the work of Handwerker, *et al*. (2007) used a similar challenge in elderly subjects (aged 51-78 years). Together, these studies indicate that breath holding can be effectively used to measure regional vascular reactivity in populations that are generally considered more difficult to train and acquire data from. Still, a better understanding of the mechanisms behind this response in healthy individuals, along with a less demanding means of achieving changes in CO_2 tensions (rather than breath holding or carbon dioxide inspiration), would be desirable for the technique to be firmly established in the clinic.

Even in healthy volunteers where we expect no gross vascular abnormalities to affect CVR, significant regional heterogeneity in BOLD signal change per unit change in end tidal CO_2 content (%BOLD/$\Delta etCO_2$) has been reported and needs to be understood (Kastrup, et al., 1998). More recently, studies by Andrade, *et al.* (2006) and Leoni, *et al.* (2008) have explored the temporal dynamics of the BOLD response to a CO_2 challenge. Specifically, trapezoidal fitting techniques were used to measure the onset time of the BOLD signal change in response

to breath holds after inspiration and expiration. Those studies relied upon averaging large numbers of voxels across vascular territory-based regions of interest, and both studies measured delays of approximately two seconds between different vascular territories but could not characterize any heterogeneity within these territories or in subcortical regions. Their results indicate that this heterogeneity in the temporal evolution of the BOLD response to hypercapnia is consistent across healthy subjects, and suggest that further exploration with better brain coverage is worthwhile. A recent study by Chang, *et al*. (2008) uses breath holding methods and correlation analysis to map latency in the BOLD response across the whole brain of healthy subjects, revealing interesting heterogeneity within vascular territories. In designing the next experiments to explore this phenomenon, it is important to recognize that standard hypercapnia techniques such as breath holding and CO_2 gas administration have prolonged BOLD effects and may not be optimal for precise analysis of the reactivity dynamics. These types of task are also difficult for many patient populations to undertake, and a less invasive and more easily executed respiratory challenge would be preferable for translation into a clinical setting.

In another fMRI study, respiration was rigorously supervised in order to obtain independent rate and depth changes resulting in variations in arterial levels of CO_2 and BOLD contrast (Birn, et al., 2008). The whole-brain BOLD response to a single deep breath was averaged across a healthy population, creating a Respiration Response Function (RRF) that describes the CVR signal change. The RRF was convolved with a respiration stimulus paradigm and compared with individual voxel timecourses. The best correlation was obtained after a variable lag parameter was introduced, and results showed optimal latencies ranging ±8 seconds. Most of this variability is reported as arising from intra-subject timing differences—further support for developing improved techniques for measuring regional heterogeneity of CVR dynamics. The authors suggest that the single-breath RRF dynamics display intriguing spatial variation that would ideally be explored on a voxel-by-voxel scale, but are unable to explore this possibility using their methods due to an insufficient signal to noise ratio.

In this study we have developed a new method for assessing regional heterogeneity in the magnitude and dynamics of the BOLD reactivity response. This novel paradigm utilizes two cycles of cued deep breaths to cause transient mild *hypocapnia*, which results in global CBF and CBV changes that can be observed using BOLD fMRI. Cued Deep Breathing (CDB) offers traditional reactivity maps of %BOLD/$\Delta etCO_2$ (mmHg) which are comparable to those created with more established methods, and the fast and robust BOLD signal response allows whole-brain temporal characterization of cerebrovascular reactivity that gives insight into dynamics that has not been previously recorded. The CDB task is not as challenging for subjects to perform as a traditional breath holding (BH) task and its non-invasive nature and minimal equipment and set-up requirements make it preferable to gas challenges (e.g. inspiration of carbon dioxide) or vasodilatory drug administration (acetozolamide etc.). These factors make CDB a more appealing choice in the laboratory where it can be instantly and easily implemented in healthy volunteers, and also may make BOLD characterization of CVR a more powerful and widely applicable clinical diagnostic tool.

In this study, we directly assess and compare the ability of CDB and BH to map the timing of the BOLD reactivity response in healthy subjects (Experiment 1). The analysis methods developed for this study allow temporal characterization throughout the brain, including subcortical gray matter, and indicate that there is interesting and consistent heterogeneity in these results. In an auxiliary experiment (Experiment 2), results from a second CDB study allowed absolute calibration of BOLD reactivity maps using end-tidal CO_2 measurements. Reactivity maps calculated from these data were compared with those created in the same subjects using a more traditional CO_2 gas inspiration technique. The results imply that this novel task may be as powerful in assessing CVR as more invasive and complex procedures.

Methods

Data acquisition

In Experiment 1, 13 healthy volunteers (aged 24-54 years, 3 female) were scanned using a 3 Tesla GE scanner equipped with a 16-channel receive coil (Nova Medical, Wilmington, MA, USA). Informed consent was obtained from all subjects, under approval of the National Institutes of Health Institutional Review Board. Subject motion was restricted with foam padding between the sides of the head and the head coil. Whole brain BOLD fMRI data were collected using a gradient echo EPI sequence (TR/TE=2000/40ms, FOV=220mm) with a voxel resolution of 2.3×2.3×5.0mm. Preprocessing steps for slice timing, motion and distortion correction were performed using SPM (Statistical Parametric Mapping, FIL, UCL, UK) and in-house programs written in Interactive Data Language (IDL, Research Systems Inc., Boulder, CO USA). A low-resolution axial Fast Spin Echo image (FOV=220mm, matrix size=256×256, 24 slices, slice thickness=5mm), and a high-resolution MPRAGE volume (Mugler and Brookeman, 1990; FOV=220mm, matrix size=256×256, 248 slices, slice thickness=0.7mm) were also acquired for assistance in registration of the subject data.

The Cued Deep Breathing (CDB) task and the CDB fMRI scan paradigm are illustrated schematically in Fig. 1. After displaying a “Ready” instruction to prepare the subject, cues to “Breathe In,” “Breathe Out,” “Breathe In,” and “Breathe Out” are displayed consecutively, in block capital letters, for two seconds each. The final cue instructs the subject to “Breathe Normally.” This challenge is repeated six times, with 90 seconds of normal breathing “recovery” in between. While the BOLD signal changes are much shorter than this window, a longer recovery interval was selected to ensure blood gas levels returned to baseline levels. A second paradigm incorporating six trials of a traditional 20-second breath holding (BH) hypercapnia task separated by 90 second periods of normal breathing was designed for comparison. Rather than instructing the subject to inhale or exhale before the hold, they were coached to cease breathing wherever they were in their natural respiratory cycle. This was done to assess the effects of breath holding independently of any preparatory breathing. The BH challenge was initiated by “Ready” and “Hold” cues displayed consecutively for two seconds each, followed twenty seconds later by a cue to “Breathe Normally.”

All instructions were projected onto a screen in the scanner room. Respiration was monitored using chest bellows incorporated into the scanner system, which were placed around the chest at the position of greatest expansion during inspiration. Although quantitative end-tidal measurements were not available, a nasal cannula was used to qualitatively monitor breathing in real-time during the scan. Two subjects that did not comply with the task were removed from the analysis. The respiratory trace was used to precisely identify the starting time of the breathing task in individual subjects, compensating for inter- and intra-subject differences in possible lag between cue and task execution. A “one-back” working memory task (Jansma, et al., 2000) was performed during the normal breathing periods and during the breath holds as part of another study; due to the consistent presence of this task throughout both paradigms we believe this should have little effect on the CVR BOLD response of interest. The scans of two further subjects experienced technical problems, resulting in ten final subject datasets being included in each of the task analyses (nine subjects in common).

Because the new CDB task presented here is not yet well examined or understood, a second study (Experiment 2) was performed using different subjects to compare the CDB hypocapnia challenge with a gas-inspiration hypercapnia paradigm using both BOLD fMRI and end-tidal gas monitoring. Eight new volunteers (aged 23-32 years, 3 female) were scanned with a 3 Tesla Siemens TIM Trio scanner also using an EPI sequence (TR/TE=1250/35ms, FOV=225mm, resolution=3.5x3.5x5mm) using foam padding to reduce head motion. In addition to the CDB paradigm, subjects also underwent a hypercapnia challenge via inspiration of carbon dioxide

enriched air. A mixture of 4% CO_2 in humidified air was supplied in two one-minute epochs using a close-fitting mask covering both the mouth and nose of the subject (8920 Series, Hans Rudolph Inc., Kansas City MO USA). These periods were interleaved with one-minute periods of normal air delivery. The mask was connected through a filter to connective tubing used to supply the gas mixtures and to a large (10cm diameter, 2m long), open-ended tube that acted both as a reservoir and as an exhaust path to minimize re-breathing of expired gases. For both paradigms, a port on the filter allowed continuous monitoring of inspired and expired respiratory composition using a carbon dioxide analyzer (Model CD-3A) and oxygen analyzer (Model S-3A) (AEI Technologies, Pittsburg, PA, USA). End-tidal values, known to well represent the arterial CO_2 and O_2 content (Robbins, et al. 1990; Young, et al. 1991), were extracted using code developed in IDL. Appropriate ethical approval for this study was obtained from the Oxfordshire Clinical Research Ethics Committee.

Data analysis

In Experiment 1, the CDB or BH BOLD signal timecourse of each voxel was interpolated using splines to a temporal resolution of 0.3 seconds. The starting times of the six breathing tasks were located using data from the respiratory belt, and the BOLD signal changes during the 50 seconds following the task onsets were averaged on a voxel-by-voxel basis. This mean response for a given voxel was then smoothed using a Gaussian kernel (3 seconds and 9 seconds FWHM were compared) and the percent change and temporal location of the signal minimum or maximum was obtained for the CDB and BH tasks, respectively. The first thresholding step removed voxels that did not show at least a 1.0% absolute BOLD signal change in response to the respiratory task. Next, the maps showing the absolute timing of the extrema of the BOLD response curve were thresholded using a 20 second window centered on the mean response for that subject. This second thresholding step removes outliers—voxels responding at the edges of the temporal window used in averaging and reflecting confounds of the analysis method and motion-related artifacts—while including enough data to accurately represent the timing heterogeneity of interest (approximately 10 second range across the brain). Finally, subject timing results were normalized using the mean response timing in voxels that remain after both thresholding steps.

The functional data were registered to the low-resolution axial Fast Spin Echo, which was in turn aligned to the high-resolution MPRAGE image (FLIRT; FSL; Jenkinson and Smith, 2001). The MPRAGE image was transformed using nonlinear registration (Andersson, et al., 2008) into MNI space (MNI152, nonlinearly derived, McConnell Brain Imaging Centre, Montreal Neurological Institute, McGill University). All volumes had non-brain matter removed using the FSL Brain Extraction Tool (Smith, 2002). Finally, these transformations were concatenated to transform the results of timing analysis into standard MNI space.

In Experiment 2, the CDB BOLD data were analyzed in an identical way to Experiment 1, although the end-tidal trace was used in lieu of respiratory belt data. The timing of the end-tidal measurements is systematically delayed by approximately 1.5 seconds due to tube lengths and flow rate, however this should not affect any relative timing characteristics in the data. The reference time, instead of using the actual cued breaths, was taken to be 8 seconds prior to the lowest end-tidal fraction CO_2 reached, which placed the mean response timing in roughly the center of our averaging window.

The 4% CO_2 gas challenge data were only analyzed for percent signal change, as the prolonged hypercapnic state does not create the sharp BOLD signal changes that allow for robust temporal characterization. The BOLD signal in the second half of each CO_2 block was averaged and compared to the signal in the baseline periods for each voxel, and normalized using the end-tidal data to create traditional reactivity maps in units of %BOLD change per mmHg etCO_2 change.

Results

In Experiment 1, volunteers reported no major difficulties with performing either the CDB or BH task, although the CDB task was generally felt to be less challenging. Both paradigms were successful in causing strong BOLD signal changes throughout gray matter such that the relative timing of the response could be characterized. Examples of motion-corrected timecourses of single gray matter voxels from both tasks are given in Fig. 2, demonstrating the typical temporal dynamics of the BOLD changes relative to the cued instructions and respiratory belt trace. Figure 3 shows examples of voxel timecourses, illustrating the BOLD response from the six trials as well as the calculated mean response and signal extremum timing, for voxels in the BH and CDB data presenting a small, typical, and large delay.

The percent BOLD signal changes were comparable between CDB and BH, noting that the hypocapnia CDB task resulted in a signal *decrease* instead of the traditional signal increase seen in hypercapnia tasks. Within gray matter, both respiratory challenges resulted in an approximate 0.5-3% absolute signal change, with even larger responses in tissue surrounding large venous vessels. Experiment 1 did not include end-tidal gas measurements and thus the data cannot be normalized to create standard %BOLD/$\Delta etCO_2$(mmHg) CVR maps. The non-normalized maps do suggest similarities between the tasks, and voxelwise correlation analysis was performed in the nine subjects that are included in both the CDB and BH datasets. Fig. 4 provides CVR maps (in units of %BOLD signal change) of four example subjects and the results of correlation analysis in 10 central slices. Most subjects show good correlation between the results of the two tasks, however the second experiment presented here is needed to quantify the true CVR maps and relationships.

The temporal evolution of the BOLD response to each task showed distinct differences beyond being simply positive or negative. In the BH data, a large BOLD signal dip was often observed following the expected positive BOLD epoch, rather than an immediate return to baseline. This may be caused by the deep recovery breaths that many of the subjects performed instead of “normal” respiration following the breath holds, possibly through the same hypocapnic mechanisms as in the CDB task. Also, in the CDB data, some voxels exhibited an initial signal *increase* before the expected dip (see Fig. 2), although this does not appear to be consistently localized to specific brain regions. A similar phenomenon has been previously observed (Birn, et al., 2008). This increase occurred near the end of the task execution and it is unclear whether it can be ascribed to motion artifacts, neuronal activity in certain respiratory-control systems, or other unaddressed phenomena. The task-related motion related to the CDB and BH paradigms appears strikingly different, as illustrated in Fig. 5. The relative mean displacement of each volume was calculated during motion correction, and the mean of this relative displacement was measured and used as a metric for the amount of motion during a given period. The CDB task was found to cause significantly more motion across the total duration of the scan, although there was significantly *less* motion during the BOLD signal change of interest.

Using the interpolation and averaging method discussed above, the strong BOLD response allowed voxelwise identification of the most prominent signal extremum and its temporal position relative to the onset of the task in both datasets. The choice of smoothing was observed to only slightly affect these results, and within a reasonable (3-9 second) range in kernel-size the regional differences in the relative timing maps did not appear to be altered. The 9 second kernel data appeared less susceptible to noisy high-frequency fluctuations and were used in further analysis. The mean timing of the BOLD extremum of each subject (following thresholding), averaged across ten subjects, was 19.6±1.8 seconds following the start of the deep breaths in the CDB task and 27.3±2.0 seconds following the start of the breath hold in the BH task. Using the whole-brain mean BOLD response in each subject, we calculated the

overall variation in the magnitude and latency of the maximal signal change following the execution of the task. The results are summarized in Table 1. There is no significant difference between the variation calculated in the BH and CDB datasets, as measured in a paired t-test.

These single-subject whole-brain maps reveal intra-subject regional differences of up to approximately 6 seconds, with an earlier response in sub-cortical gray matter, insula, and bilaterally symmetric regions of medial cortex and a delayed response in posterior regions (Fig. 6). A group map for each task was created in MNI-space by averaging each voxel that included at least four subject datasets after thresholding (Fig. 7), and this regional heterogeneity continued to be observed across normal subjects.

Experiment 2, which explores the impact of the CDB task on blood gas levels and absolute BOLD signal changes relative to a traditional hypercapnia paradigm, offers several new insights into this novel technique that could not be addressed in Experiment 1 described above. Of the eight new volunteers scanned in Experiment 2, four subjects were successful in reaching the end-tidal CO_2 changes necessary to create the strong BOLD signal changes as seen in Experiment 1. These datasets allow reactivity map comparison between CDB and CO_2 inspiration methods, and offer a “proof of principle” observation that the CDB task is a competitive method for traditional reactivity diagnostics. In these four subjects, the CDB task caused an end-tidal CO_2 decrease between 6.0±1.1 and 10.5±2.6 mmHg averaged across the six repetitions. The end-tidal levels returned to baseline after approximately three breaths. In the same subjects the 4% CO_2 challenge led to end-tidal CO_2 increases of between 3.6±1.0 and 7.9±1.2 mmHg. A comparison of the end-tidal effects in the CDB and 4% CO_2 challenge is given in Table 2. Up to a 3% increase in end-tidal O_2 fraction was measured following the CDB task, returning to baseline after approximately twenty breaths. We have calculated this physiological change to equate to a BOLD signal increase of less than 0.3%. We therefore disregard this effect in our analysis of the relatively large hypocapnia-induced BOLD signal decrease. The percent BOLD change maps were normalized to the measured end-tidal change to create reactivity maps for both the CDB and CO_2 inspiration challenges and good correlation was observed (Fig. 8).

The remaining datasets were not included in the analysis because the subjects did not reach sufficient end-tidal changes during the CDB task for accurate characterization, and no corresponding BOLD signal changes were observed. This is most likely a reflection of the constricted environment caused by the mask, filter, and tubing system: deep breathing is hindered by the resistance inherent to the filter, and while the tubing system is designed to assist in the flushing out of expired air, a portion of the expired volume will inevitably remain in the mask environment. The increased levels of CO_2 in this “dead space” is likely to prevent the subject from becoming as hypocapnic as in the initial Experiment 1, which was performed with only a nasal cannula to monitor breathing. This suggests that the CDB task, like all respiratory challenges, requires careful consideration of the scanning environment, from pre-scan training through details of task execution.

Discussion

By averaging the BOLD response to six identically cued breathing tasks, using respiratory belt and/or end-tidal gas data and spline interpolation to temporally align the data more precisely, we can characterize the timing of the BOLD reactivity signal change on a voxel-by-voxel basis, mapping parameters such as the relative timing of the signal extremum across the whole brain. The timecourse of the CDB data indicates a strong negative signal change approximately 20 seconds following the start of the 8 second breathing task, which is in reasonable agreement with the 16 second evolution of the BOLD response to a single deep breath found by Birn *et al*. (2008).

The intra-subject variation across the six trials (Tab. 1) is not negligible, although it is smaller than the range of latencies that we observe. We experimented with alternative methods of aligning the trials prior to averaging in an attempt to reduce the possible confound of this variation, using each trial's mean BOLD signal latency as a reference point for alignment. This did not improve the alignment, and actually increased the uncertainty in the mean response curve. We conclude that improvement in intra-subject variability is best addressed during data acquisition, as selecting a reference point from the data rather than from the task execution appears to add unwanted bias to our analysis. One possible way of decreasing variation across trials would involve the regulation of the depth and rate of the subject's normal breathing, although this quickly detracts from our aim of clinical feasibility: by keeping the respiratory tasks as self-directed as possible, we maintain the ease and simplicity of our paradigm. We have recently explored the differences in breath-holding BOLD signal changes when preceded by an inspired or expired breath, finding little noticeable effect of this variable (Roberts, et al., 2009). We feel that by coaching the subject to maintain “regular” normal breathing, the timing of the BH within their breathing cycle should not greatly affect results. We can hypothesize a similar phenomenon with regard to the CDB task. For researchers with highly experienced or compliant subjects, the addition of greater respiratory control (depth and rate) may prove beneficial in removing some of the effects of intra-subject variation.

We compared the results of the individual subject normalized latency maps using ROIs defined by the MNI atlas (Maziotta, et al., 2001). The results (Fig. 9) support the qualitative agreement apparent in Figure 6. The general trends in relative timing of the maximal BOLD response are similar in the BH and CDB data, and many of the regional temporal differences calculated are statistically significant. Note that the reference (zero) value in this analysis was calculated from the mean of all responsive voxels as described in the methods section, and changing this arbitrary definition could change the absolute measurements of this analysis. Still, several regions show consistent early or late responses across the population.

Because many areas of the brain may be neuronally active throughout our CVR respiratory paradigms, it is important to consider if the neuronally-driven BOLD responses are confounding our analysis of regional heterogeneity in CVR dynamics. The putamen and thalamic nuclei have been identified as functionally active during the administration of carbon dioxide, and may be responsible for gating respiratory information passed from the brain stem to the cortex (Pattinson, et al. 2009). These regions, along with regions involved in sensorimotor processing (MacKay, et al. 2003), could be potentially neuronally activated during the respiratory tasks presented in this study. However, the gross agreement of the relative timing results derived from the large negative BOLD signal change of the CDB task and the large positive BOLD change of the BH task suggests that the influence of a small BOLD signal increase due to neuronal activation on CVR characterization is minor.

The mechanism responsible for the early BOLD response seen most strikingly in the deep gray nuclei in both BH and CDB tasks is not clear. Using vascular staining techniques and scanning electron microscopy, researchers have shown the human putamen and caudate nuclei to have a notably more dense capillary network than other regions of the basal ganglia (Nonaka, et al., 1998). However, this level of density is still comparable to the capillary density in most cortical gray matter and cannot be the predominant basis for the distinct reactivity heterogeneity seen in our study. A reactivity study comparing hypocapnia and hypercapnia using PET indicated that the putamen, with the cerebellum, is the most sensitive to both conditions: the vascular responses in the putamen were large during both reactivity challenges whereas most brain regions showed a preference for either vasodilation or vasoconstriction or had a significantly smaller vascular response to all tasks (Ito, et al., 2000).

Although less striking, the group results also indicate a slightly delayed response in areas of posterior cortex, similar to the results of dynamic susceptibility contrast MRI time-to-peak maps that indicate delayed arrival of the contrast bolus in posterior cortex relative to frontal, temporal, and parietal cortices (Duyn, et al., 1994; Nasel, et al., 2000). “Passive” arterial spin labeling (ASL) arrival time maps do not show the same quick response in the basal ganglia that we observe in our BOLD reactivity data, however the group CDB map possibly suggests a delayed response in the watershed areas between vascular territories in inferior slices, in agreement with ASL arterial transit time maps in healthy subjects (Hendrikse, et al., 2008). Still, the regional heterogeneity observed in this study is not entirely explained through comparison with arterial transit and bolus time-to-peak maps; this suggests that we are measuring a more local reactivity phenomenon as well as passive blood flow properties. Although looking at a slightly different timing parameter, the relative response timing in MCA and PCA territories found in our results is in qualitative agreement with the results of Leoni *et al*. described earlier. Our analysis method allows for voxelwise characterization of this heterogeneity, in both cortical and subcortical tissues, which may offer more subtle diagnostic capabilities than the technique of averaging the BOLD response over large vascular territories, as used in the previous study.

The quality of the single-subject timing results for BH and CDB may suggest that the CDB paradigm results in less noisy mapping of this regional heterogeneity. The fast responses of the deep gray structures are more strongly defined in the CDB data, while the BH data results appear to indicate blurring of this phenomenon into nearby cortical areas and generally more extreme timing differences. These factors can be seen in the results of the ROI analysis presented in Fig. 9. The strong and short-lived BOLD changes associated after CDB may allow more precise temporal characterization relative to the greater delay of the signal changes and more gradual return to baseline seen in breath holding paradigms. Also, the BH maps prior to thresholding show voxels near the edges of the brain and at the interface of gray and white matter to have a BOLD “response” at the completion of the breath hold and the resumption of normal breathing, and are likely to be representative of task-related motion effects occurring concurrently with the reactivity-related signal change (Fig. 5). The CDB task, by comparison, does not have this confound in the timing window of interest due to the short duration of the deep breaths relative to the BOLD dynamics. The different motion associated with each task may suggest that the CDB task is better suited for analysis within a window of interest similar to the one used in this study, although it also implies that caution should be used when larger periods of a scan are desired for analysis. There is also a population of voxels in the BH data responding earlier than the majority of cortical regions that is localized to areas proximal to large sinus cavities, and these areas remain in our window of interest after thresholding steps. Both tasks have uninteresting populations of voxels that respond in the first and last seconds of the averaging window; these voxels appear to be arising from BOLD timecourses that show a continuous drift in that period rather than a clear CDB or BH related BOLD response.

Using similar tools, Chang, *et al*. (2008) have recently used maps of the latencies in BOLD signal changes during a breath holding task to improve sensitivity in characterizing functional connectivity. In their latency results they observe variation of approximately four seconds in the BOLD response delay in single subject data and regional features similar to our results, including an early response in the basal ganglia and a delayed response in the posterior cortex. This agreement exists despite differences in the parameter being measured: our study averages the voxel response to a challenge over several trials and identifies the signal extremum allowing for voxelwise variation in the amplitude *and* evolution of the signal change, whereas the study by Chang, *et al*. identifies the temporal lag that gives maximal correlation of a voxel timecourse with a mean timecourse without incorporating extra freedom in the voxel reactivity dynamics. It is not clear what is the best metric or method for measuring these delays or using CVR characteristics to correct for latency in neuronally-driven processes. The CDB data acquired

in our study does not allow for robust calculation across the whole brain of parameters other than the time-to-peak, and we used the same metric in both studies to keep our comparison consistent and fair. Further refinement of the CDB task may enable onset latency and the slope of the response to be measured. Another candidate for an informative metric may be the width of the BOLD signal change, which Birn, *et al*. (2008) noted was responsible for most of the intra-subject variation in the CVR BOLD response. More research is needed to develop more sophisticated acquisition and analysis protocols for full characterization of the voxelwise CVR BOLD signal evolution, which may enable more precise application of latency maps in increasing the sensitivity of functional studies and better understanding of the underlying physiology. Ultimately, the agreement in the latency maps of the study by Chang, et al. and the work presented here helps to validate the use of respiratory tasks in measuring small variations in BOLD dynamics.

Besides providing high-quality maps of the regional heterogeneity of reactivity timing, the CDB task is successful at obtaining %BOLD/$\Delta etCO_2$(mmHg) reactivity measurements comparable to more established methods and may prove to be applicable in a clinical setting when breath holding or CO_2 administration becomes difficult or even dangerous for certain patient populations to perform. The reduced motion associated with the CDB task during the CVR BOLD signal change, relative to the BH-related motion, may also suggest that CDB reduces noise in the analysis of the CVR response. A future study is planned to assess how the bilateral symmetry of the timing maps created with this technique in a healthy population is altered in patients with asymmetric degrees of stenosis in their internal carotid arteries. This future study will hopefully ascertain the possible merits of the methods described here in non-invasively diagnosing vascular disorders in patients, as well as provide a better understanding of the mechanisms responsible for the regional heterogeneity observed.

Acknowledgments

We thank Silvina G. Horovitz and Susan C. Fulton at the National Institutes of Health for their assistance with experiment planning and data collection.

This research was supported by the Intramural Research Program of the NIH, NINDS, EPSRC, and the UK MRC.

Bibliography

Andersson, JA.; Smith, S.; Jenkinson, M. FNIRT - FMRIB's Non-linear Image Registration Tool. 14th Annual Meeting of the Organization for Human Brain Mapping; Melbourne, Australia. 15 June - 18 June 2008; 2008. abstractAbstract 496

Andrade KC, Pontes-Neto OM, Leite JP, Santos AC, Baffa O, de Araujo DB. Quantitative aspects of brain perfusion dynamic induced by BOLD fMRI. Arq Neuropsiquiatr 2006;64:895–898. [PubMed: 17220991]

Aso K, Ogasawara K, Sasaki M, Kobayashi M, Suga Y, Chida K, Otawara Y, Ogawa A. Preoperative cerebrovascular reactivity to acetazolamide measured by brain perfusion SPECT predicts development of cerebral ischemic lesions caused by microemboli during carotid endarterectomy. Eur J Nucl Med Mol Imaging. 2008Epub ahead of print

Birn RM, Smith MA, Jones TB, Bandettini PA. The respiration response function: the temporal dynamics of fMRI signal fluctuations related to changes in respiration. NeuroImage 2008;40:644–654. [PubMed: 18234517]

Chang C, Thomason ME, Glover G. Mapping and correction of vascular hemodynamic latency in the BOLD signal. NeuroImage 2008;43:90–102. [PubMed: 18656545]

Duyn JH, van Gelderen P, Barker P, Frank JA, Mattay VS. 3D Bolus Tracking with Frequency-Shifted BURST MRI. J Comput Assist Tomogr 1994;18:680–687. [PubMed: 8089313]

Graham GD, Zhong J, Petroff OA, Constable RT, Prichard JW, Gore JC. BOLD MRI monitoring of changes in cerebral perfusion induced by acetazolamide and hypercarbia in the rat. Magn Reson Med 1994;31:557–60. [PubMed: 8015411]

Hendrikse J, Petersen ET, van Laar PJ, Golay X. Cerebral border zones between distal end branches of intracranial arteries: MR imaging. Radiology 2008;246:572–580. [PubMed: 18055872]

Handwerker DA, Gazzaley A, Inglis BA, D'Esposito M. Reducing vascular variability of fMRI data across aging populations using a breathholding task. Hum Brain Mapp 2007;28:846–859. [PubMed: 17094119]

Ito H, Yokoyama I, Iida H, Kinoshita T, Hatazawa J, Shimosegawa E, Okudera T, Kanno I. Regional differences in cerebral vascular response to PaCO2 changes in humans measured by positron emission tomography. J Cereb Blood Flow Metab 2000;20:1264–70. [PubMed: 10950385]

Jansma JM, Ramsey NF, Coppola R, Kahn RS. Specific versus nonspecific brain activity in a parametric N-back task. NeuroImage 12:688–697. [PubMed: 11112400]

Jenkinson M, Smith SM. A global optimisation method for robust affine registration of brain images. Medical Image Analysis 2001;5:143–156. [PubMed: 11516708]

Kastrup A, Li TQ, Takahashi A, Glover GH, Moseley ME. Functional magnetic resonance imaging of regional cerebral blood oxygenation changes during breath holding. Stroke 1998;29:2641–2645. [PubMed: 9836778]

Kety SS, Schmidt CF. The effects of altered arterial tensions of carbon dioxide and oxygen on cerebral blood flow and cerebral oxygen consumption of normal young me. J Clin Invest 1948;27:484–492.

Leoni RF, Mazzeto-Betti KC, Andrade KC, de Araujo DB. Quantitative evaluation of hemodynamic response after hypercapnia among different brain territories by fMRI. NeuroImage 2008;41:1192–1198. [PubMed: 18468457]

MacKay LC, Evans KC, Frackowiak RS, Corfield DR. Neural correlates of voluntary breathing in humans. J Appl Physiol 2003;95:1170–1178. [PubMed: 12754178]

Mazziotta J, et al. A probabilistic atlas and reference system for the human brain: International Consortium for Brain Mapping (ICBM). Philos Trans R Soc Lond B Biol Sci 2001;356:1293–322. [PubMed: 11545704]

Mugler JP 3rd, Brookeman JR. Three-dimensional magnetization-prepared rapid gradient-echo imaging (3D MP-RAGE). Magn. Reson. Med 1990;15:152–157. [PubMed: 2374495]

Nonaka H, Akima M, Nagayama T, Hatori T, Zhang Z. The fundamental architecture of the microvasculature of the basal ganglia and changes in senility. Neuropathology 1998;18:47–54.

Nasel C, Azizi A, Veintimilla A, Mallek R, Schindler E. A standardized method of generating time-to-peak perfusion maps in dynamic-susceptibility-contrast-enhanced MR imaging. Am J Neuroradiol 2000;21:1195–1198. [PubMed: 10954268]

Ogawa S, Lee TM, Kay AR, Tank DW. Brain magnetic resonance imaging with contrast dependent on blood oxygenation. Proc Natl Acad Sci USA 1990;87:9868–9872. [PubMed: 2124706]

Pattinson KT, Mitsis GD, Harvey AK, Jbabdi S, Dirckx S, Mayhew SD, Rogers R, Tracey I, Wise RG. Determination of the human brainstem respiratory control network and its cortical connections in vivo using functional and structural imaging. NeuroImage 2009;44:295–305. [PubMed: 18926913]

Roberts, P.; Jezzard, P.; Bulte, D. Comparison of breath holding techniques for the calibration of fMRI measurements of oxygen metabolism. 17th Annual Meeting of the International Society of Magnetic Resonance in Medicine; Honolulu, Hawaii. 18 April - 24 April 2009; 2009. abstractAbstract 711

Robbins PA, Conway J, Cunningham DA, Khamnei S, Paterson DJ. A comparison of indirect methods for continuous estimation of arterial PCO2 in men. J Appl Physiol 1990;68:1727–1731. [PubMed: 2112130]

Shiino A, Morita Y, Tsuji A, Maeda K, Ito R, Furukawa A, Matsuda M, Inubushi T. Estimation of cerebral perfusion reserve by blood oxygenation level-dependent imaging: comparison with single-photon emission computed tomography. J Cereb Blood Flow Metab 2003;23:121–135. [PubMed: 12500097]

Silvestrini M, Vernieri F, Pasqualetti P, Matteis M, Passarelli F, Troisi E, Caltagirone C. Impaired cerebral vasoreactivity and risk of stroke in patients with asymptomatic carotid artery stenosis. JAMA 2000;283:2122–2127. [PubMed: 10791504]

Smith SM. Fast robust automated brain extraction. Human Brain Mapping 2002;17:143–155. [PubMed: 12391568]

Thomason ME, Burrows BE, Gabrieli JDE, Glover GH. Breath holding reveals differences in fMRI BOLD signal in children and adults. NeuroImage 2005;25:824–837. [PubMed: 15808983]

Young WL, Prohovnik I, Ornstein E, Ostapkovich N, Matteo RS. Cerebral blood flow reactivity to changes in carbon dioxide calculated using end-tidal versus arterial tensions. J Cereb Blood Flow Metab 1991;11:1031–1035. [PubMed: 1939381]

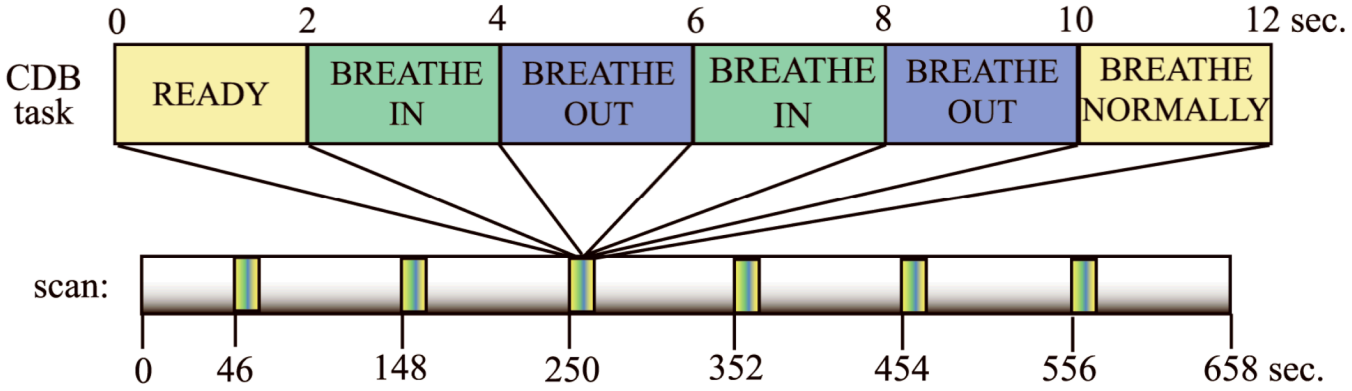

Figure 1.
Schematic of the Cued Deep Breathing (CDB) paradigm. The CDB task consists of six text cues displayed consecutively for two seconds each: Ready, Breathe In, Breathe Out, Breathe In, Breathe Out, and Breathe Normally. Scans consisted of 6 repetitions of the task, interleaved with 90 second periods of normal breathing. 329 volumes (TR=2s) were acquired, for an overall scan time of approximately 11 minutes.

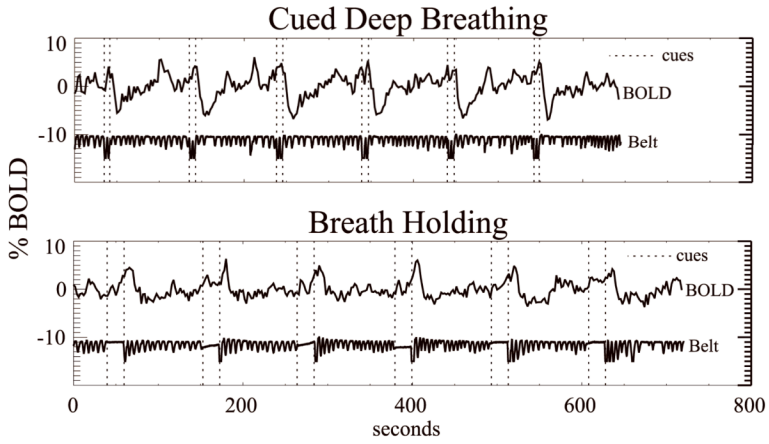

Figure 2.

Example BOLD timecourses for the Cued Deep Breathing and Breath Holding respiratory paradigms. For reference, the respiratory belt trace for each scan is included. Dashed lines indicate the timing of each of the six repetitions of the CDB or BH task.

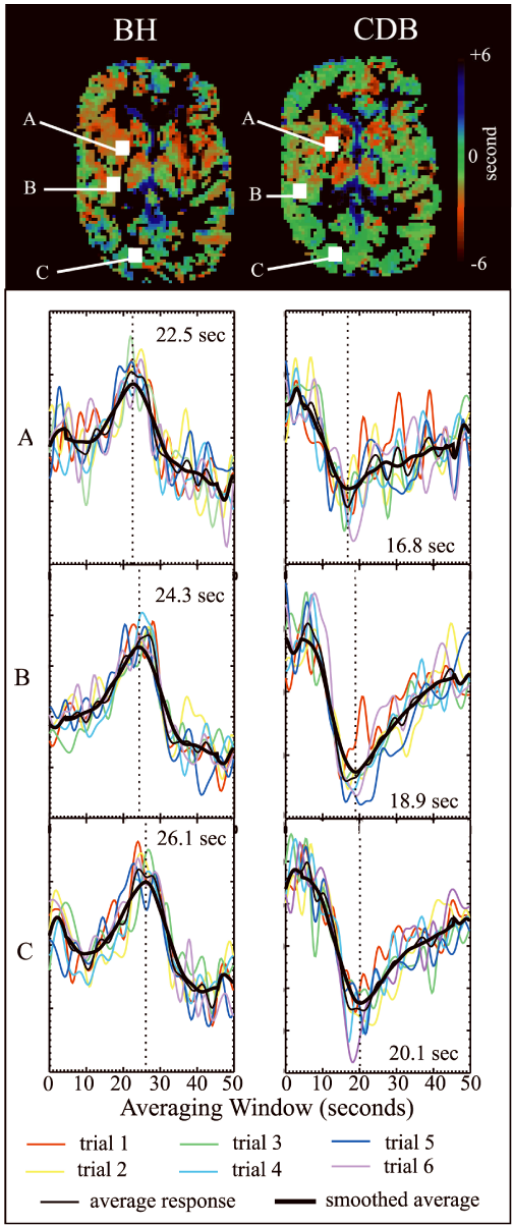

Figure 3.
Examples of trial averaging for early, intermediate, and delayed responding voxels in the BH and CDB data of a single subject. The motion corrected and detrended BOLD data for each trial is plotted (color traces) and the mean response (thin black) and smoothed mean response (thick black) are overlaid. Dashed vertical lines indicate the peak response found via our analysis methods.

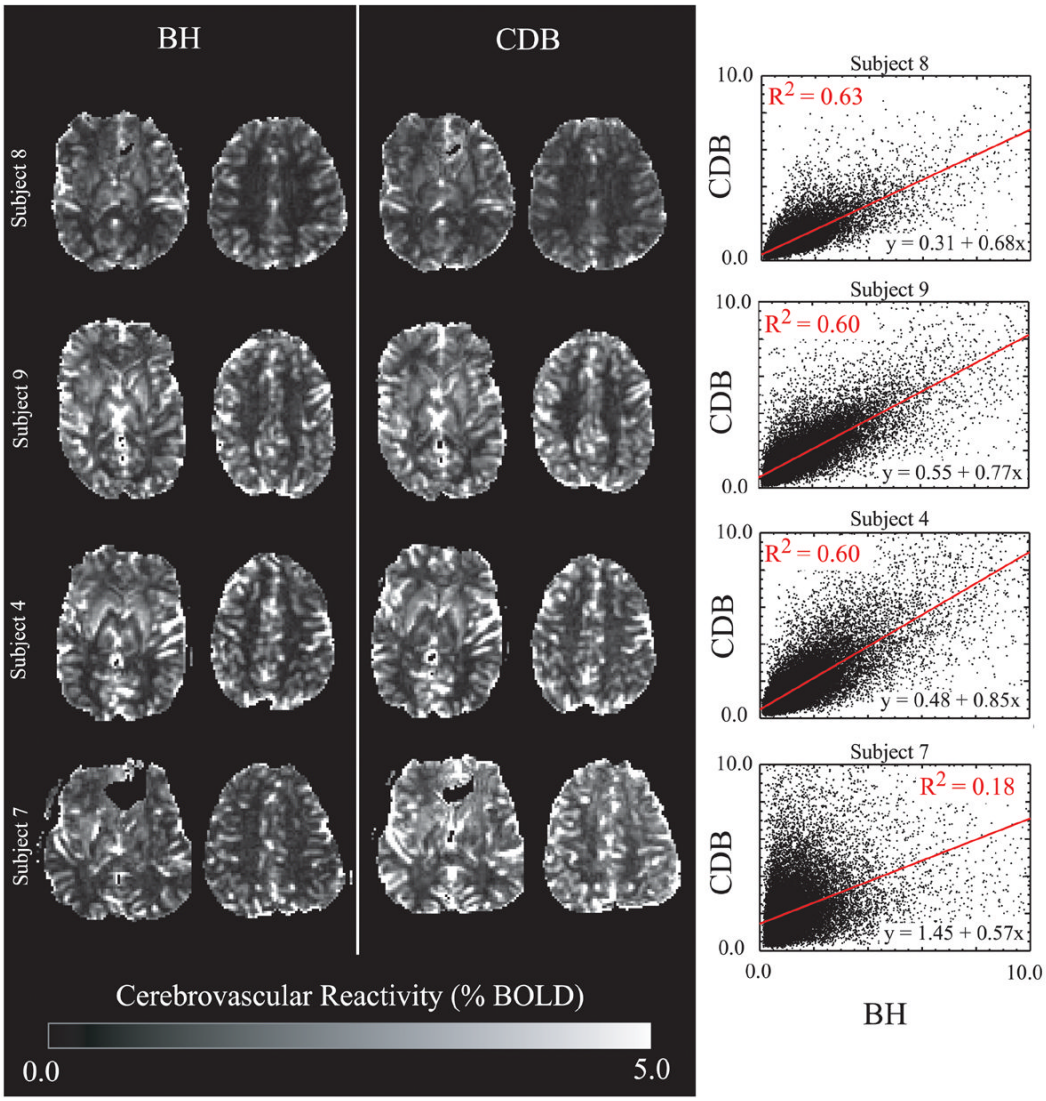

Figure 4.

Reactivity maps (in units of %BOLD signal change) resulting from the BH (left) and CDB (right) tasks in Experiment 1. Four of nine subjects are presented alongside scatterplots for comparison. The R2 correlation values of all nine subjects were calculated to be 0.55, 0.18, 0.60, 0.43, 0.18, 0.63, 0.60, 0.55, and 0.14. The three subjects with low correlation coefficients still indicate reasonable qualitative agreement between the BH and CDB results, and the poor correlation may be due to motion between scans or other confounding factors not entirely accounted for.

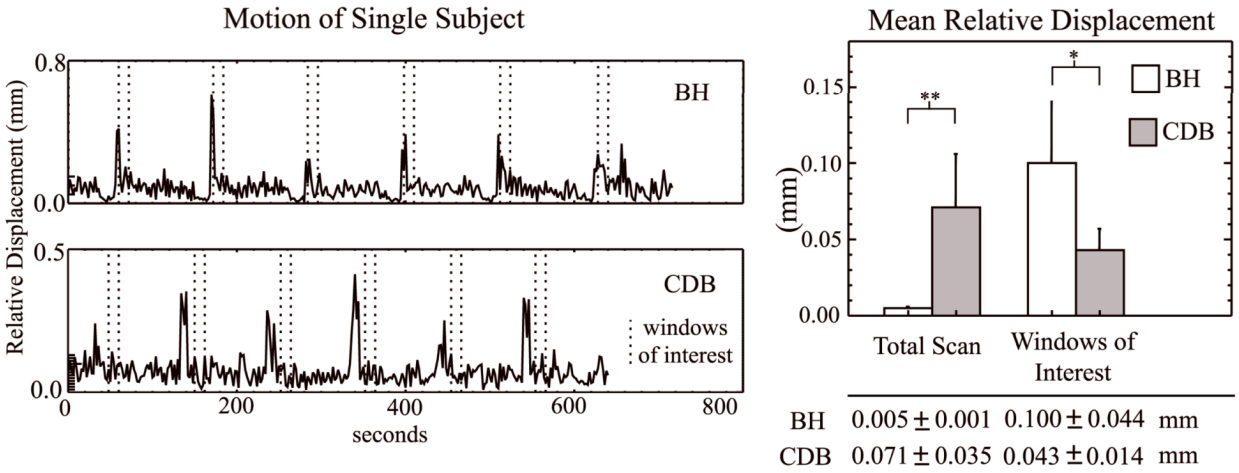

Figure 5.

Analysis of the motion associated with the BH and CDB task paradigms. The relative mean displacement of each volume is plotted, and dashed lines indicate 12 second windows centered on the mean BOLD response timing (approximately spanning the range of latencies observed in our analysis). The mean of this trace was calculated to determine the size of the subject motion. Using a paired t-test in nine subjects, we found that the CDB task was associated with greater movement across the total duration of the scan (**$p < .0005$). However, within the averaging windows of the six trials, the CDB data showed significantly *less* motion than in the BH data (*$p = 0.006$).

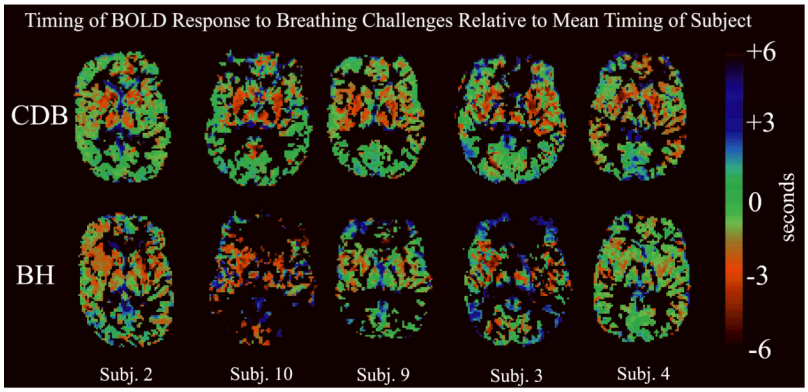

Figure 6.

Examples of matched slices from single-subject maps showing the timing of the BOLD signal extremum for the CDB (top) and BH (bottom) tasks relative to the mean timing found throughout all strongly responding voxels after temporal thresholding. Primarily these voxels are located in gray matter. A range of six seconds can be easily identified, with earlier responses (red) observed in deep gray matter structures and bilateral areas of medial cortex, and delayed responses (blue) in posterior cortical areas.

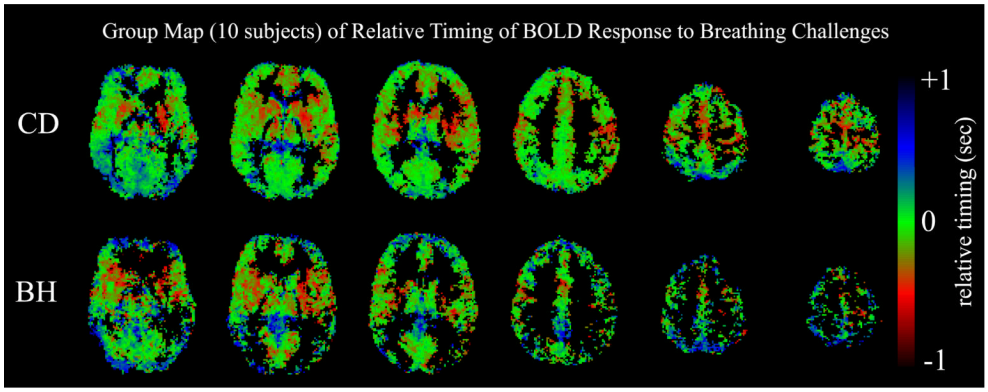

Figure 7.

Group map showing the averaged relative timing of the BOLD signal extremum for both breathing paradigms. Single subject maps, as illustrated in Fig. 3, were aligned to MNI space. All voxels in which at least 4 subjects had a strong (>1.0% BOLD) response were included.

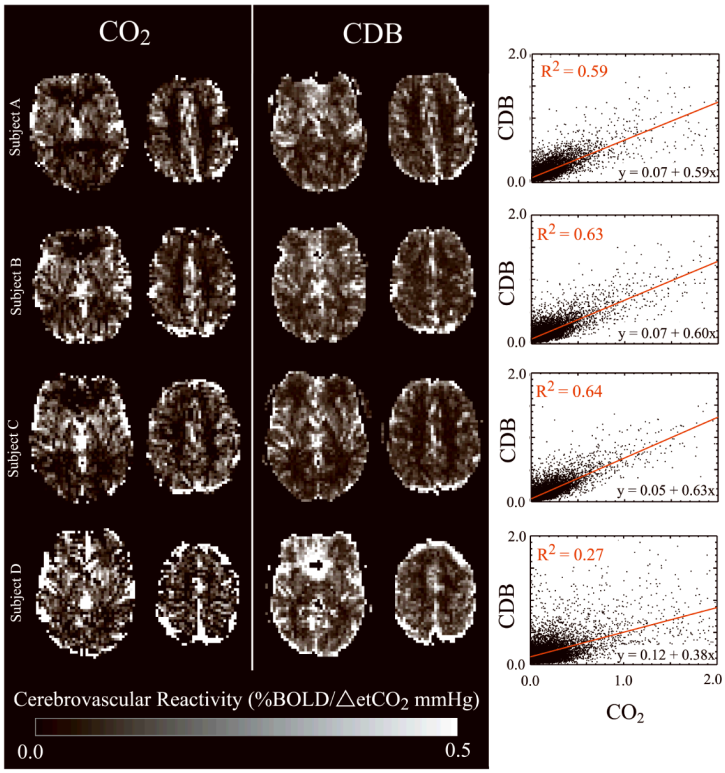

Figure 8.
Normalized reactivity maps (%BOLD/ΔetCO_2) from Experiment 2 for both the traditional CO_2 gas administration challenge (left) and CDB paradigm (right). Scatterplots relating these CVR data show good correlation between the results of the two challenges.

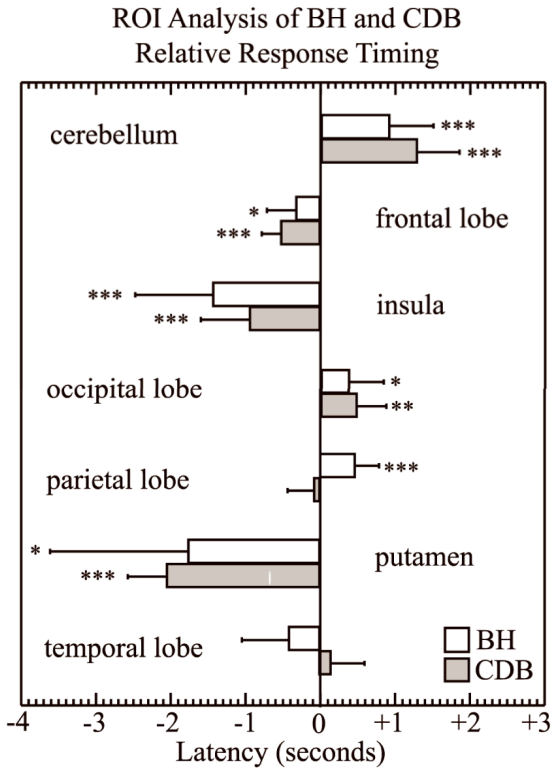

Figure 9.

Comparison of the relative BOLD signal timing in BH and CDB data in ten subjects. Regions of interest were obtained from the MNI atlas, and t-tests were performed to determine statistically significant nonzero latencies (*p < .05 , **p < .01 , ***p < .005). The subject mean value has been defined as the mean response in all responding voxels, and there exist equally valid alternative measures that may give slightly offset values for this analysis. However, this would not detract from the trend in regional heterogeneity observed.

Table 1

Intra-subject variability of the BOLD response to BH and CDB across the 6 trials, calculated using the global mean BOLD signal

Subj.	BH magnitude stdev (units of % signal change)	CDB magnitude stdev (units of % signal change)	BH timing stdev (seconds)	CDB timing stdev (seconds)
1	-	0.22	-	1.46
2	0.26	0.39	2.92	1.84
3	0.21	0.17	1.25	2.23
4	0.37	0.69	3.00	2.23
5	0.17	-	4.04	-
6	0.19	0.21	4.46	1.35
7	0.19	0.14	1.59	0.35
8	0.10	0.22	3.78	1.49
9	0.25	0.21	0.70	2.01
10	0.30	0.35	4.70	3.16
11	0.22	0.32	1.77	2.07
Mean	0.23 ± 0.08	0.30 ± 0.17	2.69 ± 1.44	1.86 ± 0.77

Table 2

End-tidal CO_2 levels in baseline conditions and CDB and gas administration tasks (mmHg)

Subj	CDB Paradigm		CO_2 Paradigm	
	Baseline (mmHg)	CDB (mmHg)	Baseline (mmHg)	4% CO_2 (mmHg)
A	39.0±2.0	28.4±1.7	43.0±1.3	49.9±0.7
B	37.5±0.6	31.4±1.0	36.6±1.1	43.1±0.4
C	44.6±1.0	34.6±1.5	44.1±0.8	47.7±1.0
D	40.9±1.4	32.5±3.0	40.5±1.0	48.4±0.7